Au/TiO2/Au as a Plasmonic Coupling Photocatalyst

ARTICLE *in* THE JOURNAL OF PHYSICAL CHEMISTRY C · MARCH 2012

Impact Factor: 4.77 · DOI: 10.1021/jp212303q

THE JOURNAL OF PHYSICAL CHEMISTRY C

Article

pubs.acs.org/JPCC

Au/TiO_2/Au as a Plasmonic Coupling Photocatalyst

Hua Wang,[†] Tingting You,[†] Weiwei Shi,[†] Jinghong Li,*[,‡] and Lin Guo*[,†]

[†]School of Chemistry and Environment, Beihang University, Beijing 100191, People's Republic of China

[‡]Department of Chemistry, Beijing Key Laboratory for Microanalytical Methods and Instrumentation, Tsinghua University, Beijing 100084, People's Republic of China

ABSTRACT: The enhanced near-field amplitude of localized surface plasmon resonance in the proximity of metal nanoparticles can boost the photocatalytic activity of the neighboring semiconductor, which has been proven and has attracted wide interest recently. Since the plasmon resonance energy strongly depends on the metal particle size and shape, interparticle spacing, and dielectric property of the surrounding medium, it is available to improve the photocatalytic activity of the neighboring semiconductor by designing and synthesizing targeted metal nanoparticles or assembled nanostructures. In this paper, we propose a Au/TiO_2/Au nanostructure with the thickness of the middle layer TiO_2 nanosheets around 5 nm, which satisfies the distance needed for the coupling effect between the opposite and nearly touching Au nanoparticles, and thus, it can be used as a "plasmonic coupling photocatalyst". Compared with the bare TiO_2 nanosheet films, the photocurrent density of this favorable nanostructure exhibited a significant improvement in the visible region. The three-dimensional finite-difference time domain was used to quantitatively account for the electromagnetic enhancement of this Au/TiO_2/Au heterostructure and substantiated the plasmonic enchancement photocatalytic mechanism further.

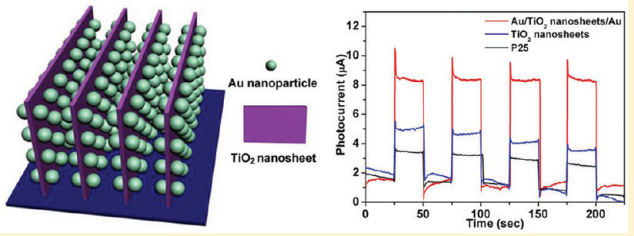

1. INTRODUCTION

With sustainable energy production and environmental protection emerging as the top issues for humanity, semiconductor photocatalysts have received much attention for their potential applications in water splitting and photodegradation of organic pollution using solar energy.[1−6] Among various photocatalysts, TiO_2 has been most widely investigated due to its low cost and excellent chemical and photochemical stability. However, its large band gap requires high-energy ultraviolet (UV) light, which only accounts for a small fraction (<4%) of the total solar spectrum reaching the surface of the earth, while its low separation efficiency of the photoinduced electron−hole pairs also hampers its practical application.[7−9] Crystal growth control, doping, and heterostructuring of the TiO_2 photocatalyst are the three main strategies to improve its photocatalytic activity.[10−13]

Compared to the single-phase TiO_2 photocatalyst, TiO_2-based heterostructures can spread the light-response range to the visible region and improve the charge separation and transfer properties by combining different electronic structures, thus promoting photocatalytic efficiency.[12−14] Sensitization with a narrow band gap semiconductor and noble metal decoration are generally used to construct TiO_2-based heterostructures.[7−9] The loading of a noble metal on the surface of TiO_2 can improve the photocatalytic properties in two aspects. On one hand, the deposited noble metal can act as an electron trap aiding electron−hole separation and thus improve the quantum yield.[14−16] On the other hand, the surface plasmon resonance (SPR) effect, defined as the collective coherent oscillation of the free electrons on noble metal nanostructures induced by visible light irradiation, can enhance the localized electric field in the proximity of the metal particles, whereas the interaction of localized electric fields with a neighboring semiconductor allows for the facile formation of electron−hole (e^-−h^+) pairs in the near-surface region of the semiconductor.[17−20] Recently, the SPR effect of a noble metal to boost the photoelectrochemical properties has attracted attention due to its potential application future. Both Awazu and Linic have proved the plasmonic enhancement photocatalytic mechanism by isolating Ag nanoparticles using SiO_2 and poly(vinylpyrrolidone) (PVP) as shells, respectively.[17,18] Liu et al. proposed an effective plasmonic photocatalyst for water splitting under visible illumination by integrating Au nanoparticles with doped TiO_2 nanotubes.[21] Furthermore, the plasmon resonance wavelength and intensity strongly depend on the particle size and shape, interparticle spacing, and dielectric property of the surrounding medium.[22−26] However, efforts through adjusting these factors of noble metal nanostructures to enhance the plasmon resonance energy and therefore to improve the photocatalytic activities of semiconductors are rare.

Great experimental and theoretical efforts have powerfully confirmed that the "hot spot", the gap region between the nearly touching metal particles, can induce several orders of magnitude enhancement of local field effects in comparison with those of isolated metal particles.[27,28] Recently, many

Received: December 21, 2011
Revised: February 16, 2012
Published: March 6, 2012

assembled and particularly shaped metal nanoparticles possessing a great quantity of local hot spots have been employed for surface-enhanced Raman spectroscopy (SERS) studies, and large SERS enhancement has been obtained.[29−32] Inspired by these results, we designed and synthesized a Au/TiO_2 sheet/Au nanostructure, as shown in Scheme 1. In the as-prepared

Scheme 1. Schematic Structure of Au/TiO_2 Nanosheets/Au on a Ti Foil[a]

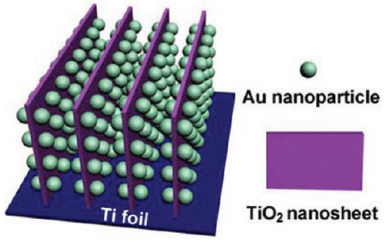

[a]TiO_2 nanosheets are grown directly on a Ti foil, and Au nanoparticles are deposited on both sides of these nanosheets.

structure, TiO_2 nanosheets are grown directly on a Ti foil, and Au nanoparticles are deposited on both sides of these nanosheets. The thickness of the TiO_2 nanosheets between the Au interparticles is only about 5 nm, which satisfies the space needed for plasmonic coupling resonance between the interparticles, and thus, the as-prepared nanostructure can be used as a "plasmonic coupling photocatalyst" to boost the photocatalytic activity by taking advantage of the hot spot effect. Compared with the bare TiO_2 nanosheet films, the photocatalytic activity of this Au/TiO_2/Au nanostructure shows a significant improvement under visible light illumination. The three-dimensional finite-difference time domain (3D FDTD) method was used to quantitatively account for the electromagnetic enhancement between the illuminated interparticles and to investigate the underlying photocatalytic enhancement mechanism of this Au/TiO_2/Au heterostructure.

2. EXPERIMENTAL SECTION

2.1. Preparation of the Au/TiO_2 Nanosheet/Au Photocatalyst. The perpendicular TiO_2 nanosheet films were prepared using hydrothermal synthesis reported previously.[33] Briefly, one piece of titanium foil (1 cm × 2 cm) was cleaned in a 10% aqueous HF solution for 10 s to remove surface oxide. After the HF treatment, the titanium foil was flushed with a large amount of water and ethanol, and then it was placed at an angle against the wall of the Teflon lining with 40 mL of aqueous ammonia solution (25−28%, Beijing Chemical Co.) and kept at 100 °C for 4 days. After the hydrothermal treatment, the as-prepared ammonium titanite films on Ti foils were then sintered at 500 °C in air for 4 h and transformed to TiO_2 films. The Au/TiO_2 nanosheet/Au photocatalyst was fabricated by sputtering for 20 s using a Au sputtering system (SBC-12, KEYI Technology Development Ltd., China, p = 0.12 mbar, 5 mA). P25 films on Ti foils were prepared following our previous work.[5,14] Typically, the paste was obtained by mixing ethanol and the P25 powder homogeneously (150 mg/mL). The P25 films were prepared by spreading the TiO_2 paste on the Ti foils with a glass rod using pieces of adhesive tape as spacers and then heated at 450 °C.

2.2. Characterization. The morphology of the sample was studied by a field-emission gun scanning electron microscope (Hitachi S-4800, 5 KV). Transmission electron microscopy (TEM) and high-resolution TEM (HRTEM) investigations were carried out with a JEOL JEM-2100F microscope. The TiO_2 sample was detached from the Ti foil substrate, then dispersed in ethanol, and dropped onto a carbon film supported on a copper grid. Diffuse reflectance absorption spectra of P25 films and TiO_2 nanosheets films with and without Au nanoparticles were recorded in the range from 300 to 800 nm using a Hitachi U-3010 spectrophotometer with Ti foils as the references.

2.2. Photoelectrochemical Measurements. The photocatalytic water splitting reaction was measured with an electrochemical analyzer (CHI 660C, CH Instruments, Austin, TX) in a standard three-electrode configuration. The as-prepared TiO_2 films were used as the working electrode, a glassy carbon electrode was used as the counter electrode, and a saturated Ag/AgCl electrode was used as the reference electrode. KOH aqueous solution (1 M) was used as the electrolyte. The working electrode was illuminated within an area of about 1 cm^2 at zero bias voltage versus the Ag/AgCl electrode under UV (254 nm, 3 mW/cm^2) and solar-simulated (AM 1.5 G filtered, 100 mW/cm^2, 69911, Oriel) light sources with a UV cutoff filter (providing visible light with $\lambda \geq 400$ nm).

Photocurrent action spectra were obtained with a 500 W xenon lamp with a monochromator. The photoelectrodes were illuminated within an area of about 0.12 cm^2 by incident light in a 1 M KOH solution, and a platinum wire was used as the counter electrode. The generated photocurrent signals were collected by using a lock-in amplifier (Stanford Research Systems SR830 DSP) synchronized with a light chopper (Stanford Research Systems SR540). The monochromatic illuminating light intensity was about 15 μW/cm^2 at 475 nm estimated with a radiometer (Photoelectronic Instrument Co. IPAS).

3. RESULTS AND DISCUSSION

The perpendicular TiO_2 nanosheet films were prepared using hydrothermal synthesis reported by Zhou's group.[33] Typically, the ammonium titanate films were first produced by hydrothermal treatment with bare Ti foil in ammonium solution following the equation

$$n\mathrm{Ti} + 2\mathrm{NH_4OH} + (2n-1)\mathrm{H_2O} \rightarrow (\mathrm{NH_4})_2\mathrm{Ti}_n\mathrm{O}_{2n+1} + 2n\mathrm{H_2}$$

Then the obtained ammonium titanate films were sintered at 500 °C in air for 4 h and transformed into TiO_2 films. Parts A and B of Figure 1 are typical SEM images of the as-prepared TiO_2 films, and it can be seen that the films are composed of perpendicular TiO_2 nanosheets with an average thickness of about 5 nm (the film thickness is around 250 nm). Figure 1C is the TEM image of the TiO_2 nanosheets, which shows a two-dimensional and nearly transparent nanostructure, indicating the nanosheets are very thin. The corresponding HRTEM image is shown in Figure 1D, which shows the lattice fringes with interplanar spacings d_{101} = 0.350 nm and d_{112} = 0.231 nm consistent with the anatase phase (JCPDS card no. 21-1272). The Au particles were deposited on the surface of the TiO_2 sheets by electron beam evaporation. As shown in Figure 1E,F, the islandlike Au nanoparticles with an average particle size of ~15 nm were dispersed on both sides of the perpendicular TiO_2 nanosheets, and the as-prepared Au/TiO_2/Au nanostruc-

dx.doi.org/10.1021/jp212303q | J. Phys. Chem. C 2012, 116, 6490−6494

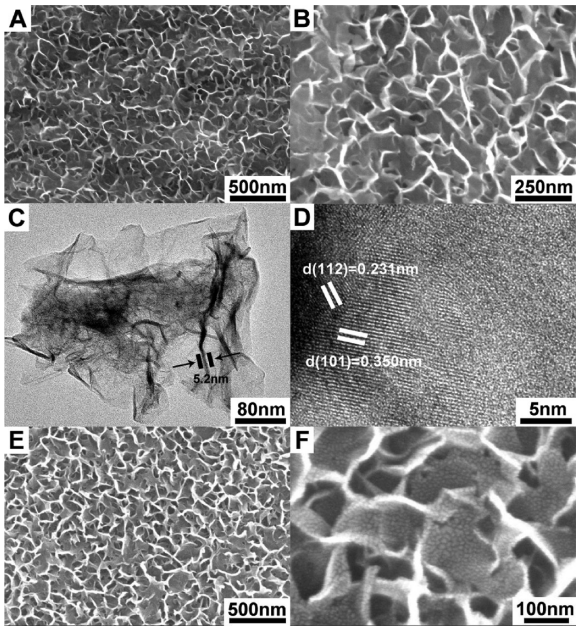

Figure 1. SEM images of bare TiO_2 nanosheets grown on Ti foils at (A) low and (B) high magnifications. TEM (C) and HRTEM (D) images of bare TiO_2 nanosheets. SEM images of as-prepared Au/TiO_2 nanosheets/Au on Ti foils at (E) low and (F) high magnifications.

ture is in line with the tentative structure illustrated in Scheme 1.

Diffuse reflectance absorption spectra of commercial P25 on Ti foils and TiO_2 nanosheets with and without Au nanoparticles are shown in Figure 2. The P25 films can absorb

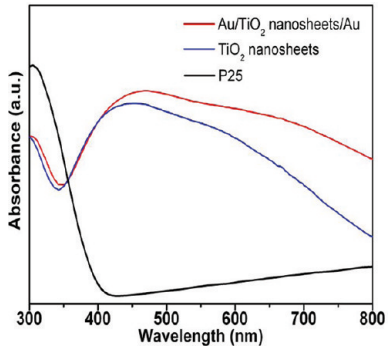

Figure 2. Diffuse reflectance absorption spectra of bare TiO_2 nanosheets, Au/TiO_2 nanosheet/Au, and P25 films on Ti foils. The spectra are referenced to Ti foils.

ultraviolet light with wavelengths smaller than 410 nm due to the composition of anatase- and rutile-phase TiO_2 nanoparticles. However, the TiO_2 nanosheet films show obvious absorption in the visible light region, which can be attributed to the N-doping and other impurity doping during the hydrothermal and sintering process.[34−37] Meanwhile, the Au-deposited TiO_2 nanosheet films exhibit increased light absorption intensity due to the SPR effect of Au nanoparticles. The visible light absorption of TiO_2 nanosheet films with and without Au nanoparticles is expected to facilitate their application in practical water splitting and environmental remediation.

To elucidate the effect of the Au nanoparticles on the photocatalytic activity of the $Au/TiO_2/Au$ composite nanostructure, the photocurrent response of the TiO_2 nanosheets with and without Au nanoparticles is measured under on−off illumination with the UV and visible light, respectively. For comparison experiments, the photocatalytic activities of commercial P25 films on Ti foils were also tested. As shown in Figure 3A, the photocurrent densities of the TiO_2

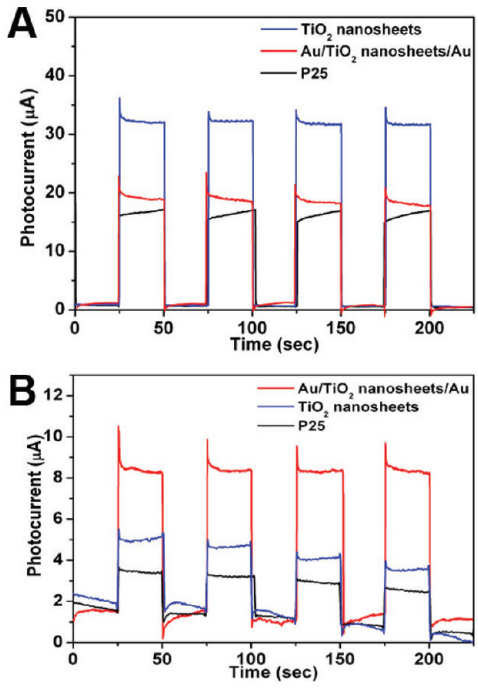

Figure 3. Photocurrent of bare TiO_2 nanosheets, Au/TiO_2 nanosheet/Au, and P25 film photoelectrodes irradiated with (A) UV (λ = 254 nm, 3 mW/cm^2) and (B) visble (λ > 400 nm, 100 mW/cm^2) light. The photoelectrodes were measured at zero bias voltage versus Ag/AgCl in 1 M KOH aqueous solution.

nanosheets both with and without Au nanoparticles are higher than those of P25 films, which may result from the superior electron transfer properties of the TiO_2 nanosheets grown directly on Ti foils, while the perpendicular TiO_2 nanosheets facilitate ion diffusion of the electrolyte. Under further observation, it can be seen that the photocurrent densities of $Au/TiO_2/Au$ films present an obvious reduction compared with those of bare TiO_2 nanosheets, which can be explained by the reduction in UV light absorption of TiO_2 shielded by Au nanoparticles, as shown in Figure 3B. Interestingly, the results are just contrary under visible light illumination, and the photocurrent density of $Au/TiO_2/Au$ shows a significant enhancement compared with those of bare TiO_2 nanosheets. Many research groups attributed these enhanced photoelectrochemical properties to the plasmonic heating effect of the Au nanoparticles or the charge transfer mechanism by regarding Au nanoparticles as a kind of semiconductor similar to a sensitizer in a dye-sensitized solar cell (DSSC), but these explanations seem unreasonable.[21] At present, the mechanism in which the SPR effect of a noble metal improves the light absorption of TiO_2 and facilitates the selective formation of electron−hole pairs in the near-surface region of the neighboring semiconductor has been accepted by more and more people.[17−19]

Figure 4A shows the photocurrent action spectra of the P25 film and TiO_2 nanosheets with and without Au nanoparticle

dx.doi.org/10.1021/jp212303q | J. Phys. Chem. C 2012, 116, 6490−6494

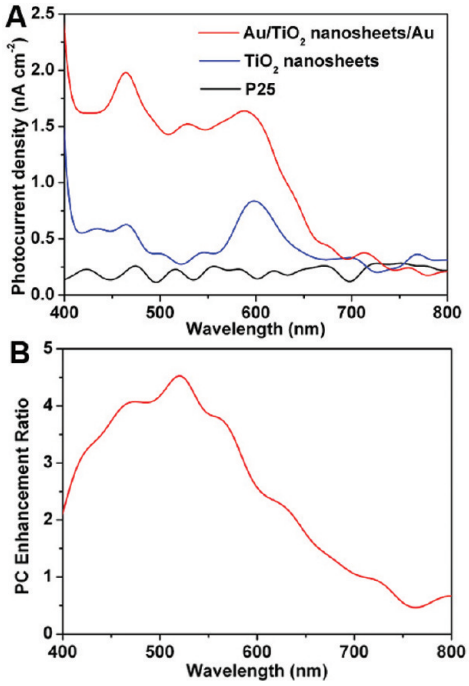

Figure 4. Photocurrent spectra of bare TiO_2 nanosheets, Au/TiO_2 nanosheet/Au, and P25 film photoelectrodes (A) and photocurrent enhancement ratio spectrum of Au/TiO_2 nanosheet/Au compared with bare TiO_2 nanosheet photoelectrodes (B). The monochromatic illuminating light intensity was about 15 $\mu W/cm^2$ at 475 nm. The illumination area of the electrodes was about 0.12 cm^2.

photoelectrodes. It can be seen that the P25 film shows nearly no photocurrent action in the visible light region, whereas the bare TiO_2 nanosheets exhibit obvious photocurrent action under visible light illumination, which should be mainly attributed to N-doping and other impurity doping to spread light absorbance and is consistent with the diffuse reflectance absorption spectroscopy analysis. Meanwhile, the Au/TiO_2/Au photoelectrode shows further photocurrent improvement in the range from 400 to 650 nm compared with the bare TiO_2 nanosheet film, which suggests a significantly enhanced overall efficiency in the visible light region and accounts for the aforementioned photocurrent response under on-off illumination. Furthermore, the photocurrent improvement ratio of the Au/TiO_2/Au photoelectrode compared with the bare TiO_2 nanosheet photoelectrode was about 3-fold on average in the wavelength region from 400 to 650 nm, as shown in Figure 4B. The superior photoelectrochemical properties achieved here should be mainly attributed to the localized electric field improvement of the neighboring TiO_2 by the SPR effect of the Au nanoparticles, and especially, the hot spot resulting from the coupling effect of the opposite Au nanoparticles can magnify the localized electric fields significantly due to this favorable Au/TiO_2/Au nanostructure.

To further understand the photocatalytic mechanism of the Au/TiO_2 nanosheet/Au photoelectrode, the 3D FDTD method was used to calculate the electromagnetic field distribution around the light-illuminated Au nanoparticles by solving Maxwell's equations.[38−40] In the FDTD approach both space and time are divided into discrete segments. The space is segmented into cells, which are known as Yee cells. On the basis of the Yee cell, electric fields and magnetic fields are calculated alternately step by step at sequenced time and space segments. To approximate the experimental condition, a model in this work was constituted with a 100 nm × 100 nm × 5 nm TiO_2 slab and 50 gold nanospheres with a diameter of 15 nm, as shown in Figure 5A. An incident plane wave was propagated

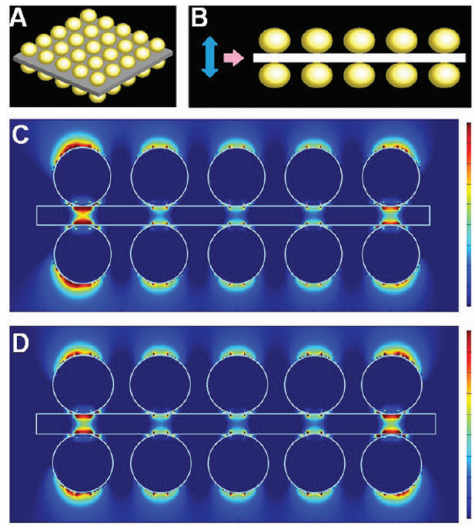

Figure 5. 3D FDTD simulated model (A, B) and electric field enhancement distribution (C, D) of the Au/TiO_2 nanosheet/Au photoelectrode: (C) electric field intensity distribution of the *yz* plane, (D) electric field intensity distribution of the *xz* plane. The scale bar is 10. The incident light is along the *z* axis.

from the *y* axis and polarized along the *z* axis as described in Figure 5B, and the wavelength was set to be 600 nm. The data for dielectric constants were from Tompkins[41] and Johnson and Christy[42] for TiO_2 and Au, respectively. The Yee cell size in FDTD simulation was carefully considered to meet the accuracy needed by both wavelength and object parameters.

The calculated electric field of the Au/TiO_2/Au nanostructure is shown in Figure 5C,D, and the corresponding maximum electric field intensity enhancement is 38-fold. The significant electric field enhancement should result from the polarization-dependent coupling effect between opposite Au nanospheres along the *z* axis. The average electric field enhancement of the whole stimulation area is 6-fold, which is a little higher than the average photocurrent improvement ratio observed experimentally, suggesting the experimental conditions can be optimized further. The average electric field intensity enhancement near nanoparticles is around 3-fold, which agrees well with the average photocurrent improvement ratio observed experimentally. As mentioned above, the plasmon resonance energy strongly depends on the particle size and shape and interparticle spacing of noble metal nanoparticles, so through design and synthesis of favorable metal nanparticles or assembled nanostructures the photocatalytic properties of semiconductors can be adjusted and improved. Our above results just give one example to enhance the photocatalytic activity of TiO_2 by designing and synthesizing a Au/TiO_2/Au nanostructure to utilize the coupling effect of opposite and nearly touching Au nanoparticles. Meanwhile, first modifying TiO_2 itself to spread light absorbance to the visible region by deep doping or sensitizing with a narrow band semiconductor and then coupling it with a plasmonic noble metal to boost the localized electric field intensity should be another significant way to improve its photocatalytic activity.

dx.doi.org/10.1021/jp212303q | J. Phys. Chem. C 2012, 116, 6490−6494

4. CONCLUSIONS

In summary, we proposed a Au/TiO_2/Au nanostructure grown directly on Ti foils as a plasmonic coupling photocatalyst. Compared with the bare TiO_2 nanosheet films, the photocurrent improvement ratio of this favorable nanostructure is about 3-fold on average in a wide visible light region from 400 to 650 nm, which shows an exciting future for practical water splitting. The improved photocatalytic activity is mainly attributed to the local electric field enhancement on the TiO_2 surface due to the plasmonic coupling resonance effect of the nearly touching and opposite Au nanoparticles, which has been quantitatively interpreted by the FDTD simulations. Our experimental results and fundamental understanding demonstrate that it is feasible to improve the photocatalytic activity of the neighboring semiconductor by adjusting the assembly mode of Au nanoparticles, whereas the plasmon resonance energy of the metal particle also strongly depends on other factors, such as the particle size and shape, as well as the dielectric properties of the surrounding medium. Meanwhile, first modifying TiO_2 itself and then coupling it with a plasmonic noble metal should be another significant way to improve its photocatalytic activity. Therefore, our work presents just the tip of the iceberg, which should inspire us to investigate other ways to improve the photocatalytic activities of semiconductors.

AUTHOR INFORMATION

Corresponding Author

*Phone and fax: +86-10-82338162. E-mail: jhli@mail.tsinghua.edu.cn (J.L.); guolin@buaa.edu.cn (L.G.).

Notes

The authors declare no competing financial interest.

ACKNOWLEDGMENTS

This work was supported by the National Basic Research Program of China (Grants 2011CB935704 and 2010CB934700), the National Natural Science Foundation of China (Grants 11079002, 50725208, and 20973019), the Tsinghua University Initiative Scientific Research Program, the Innovation Foundation of BUAA for PhD Graduates (BUAA = Beijing University of Aeronautics and Astronautics), and a Fellowship for Excellent Doctoral Student granted by the China Ministry of Education.

REFERENCES

(1) Fujishima, A.; Honda, K. *Nature* **1972**, *238*, 37.
(2) Kudo, A.; Kato, H.; Nakagawa, S. *J. Phys. Chem. B* **2000**, *104*, 571.
(3) Zou, Z.; Ye, J.; Sayama, K.; Arakawa, H. *Nature* **2001**, *414*, 625.
(4) Li, J. H.; Zhang, J. Z. *Coord. Chem. Rev.* **2009**, *253*, 3015.
(5) Zhang, H.; Lv, X.; Li, Y. M.; Li, L. M.; Li, J. H. *ACS Nano* **2010**, *4*, 380.
(6) Wang, G.; Lu, W.; Li, J. H.; Choi, J.; Jeong, Y.; Choi, S. Y.; Park, J. B.; Ryu, M. K.; Lee, M. *Small* **2006**, *2*, 1436.
(7) Liu, G.; Wang, L. Z.; Yang, H. G.; Chen, H. M.; Lu, G. Q. *J. Mater. Chem.* **2010**, *20*, 831.
(8) Chen, X. B.; Mao, S. S. *Chem. Rev.* **2007**, *107*, 2891.
(9) Wang, H.; Bai, Y. S.; Zhang, H.; Zhang, Z. H.; Li, J. H.; Guo, L. *J. Phys. Chem. C* **2010**, *114*, 16451.
(10) Han, X. G.; Kuang, Q.; Jin, M. S.; Xie, Z. X.; Zheng, L. S. *J. Am. Chem. Soc.* **2009**, *131*, 3152.
(11) Liu, Y.; Li, Li; Wang, M. J.; Li, Z. Y.; Liu, H. T.; He, P.; Yang, X. R; Li, J. H. *Cryst. Growth Des.* **2005**, *5*, 1643.
(12) Tada, H.; Mitsui, T.; Kiyonaga, T.; Akita, T.; Tanaka, K. *Nat. Mater.* **2006**, *5*, 782.
(13) Baker, D. R.; Kamat, P. V. *Adv. Funct. Mater.* **2009**, *19*, 805.
(14) Zhang, H.; Wang, G.; Chen, D.; Lv, X. J.; Li, J. H. *Chem. Mater.* **2008**, *20*, 6543.
(15) Paramasivam, I.; Macak, J. M.; Schmuki, P. *Electrochem. Commun.* **2008**, *10*, 71.
(16) Armelao, L.; Barreca, D.; Bottaro, G. J.; Gasparotto, A.; Maccato, C.; Maragno, C.; Tondello, E.; Stangar, U. L.; Bergant, M.; Mahne, D. *Nanotechnology* **2007**, *18*, 375709.
(17) Awazu, K.; Fujimaki, M.; Rockstuhl, C.; Tominaga, J. J.; Murakami, H.; Ohki, Y.; Yoshida, N.; Watanabe, T. *J. Am. Chem. Soc.* **2008**, *130*, 1676.
(18) Ingram, D. B.; Linic, S. *J. Am. Chem. Soc.* **2011**, *133*, 5202.
(19) Thimsen, E.; Formal, F. L.; Grätzel, M.; Warren, S. C. *Nano Lett.* **2011**, *11*, 35.
(20) Xu, Z. H.; Li, C. X.; Kang, X. J.; Yang, D. M.; Yang, P. P.; Hou, Z. Y.; Lin, J. *J. Phys. Chem. C* **2010**, *114*, 16343.
(21) Liu, Z. W.; Hou, W. B.; Pavaskar, P.; Aykol, M.; Cronin, S. B. *Nano Lett.* **2011**, *11*, 1111.
(22) Feldstein, M. J.; Keating, C. D.; Liau, Y. H.; Natan, M. J.; Scherer, N. F. *J. Am. Chem. Soc.* **1997**, *119*, 6638.
(23) El-Sayed, M. A. *Acc. Chem. Res.* **2001**, *34*, 257.
(24) Lin, S.; Li, M.; Dujardin, E.; Girard, C.; Mann, S. *Adv. Mater.* **2005**, *17*, 2553.
(25) Feng, X.; Ruan, F.; Hong, R.; Ye, J.; Hu, J.; Hu, G.; Yang, Z. *Langmuir* **2011**, *27*, 2204.
(26) Rycenga, M.; Cobley, C. M.; Zeng, J.; Li, W.; Moran, C. H.; Zhang, Q.; Qin, D.; Xia, Y. N. *Chem. Rev.* **2011**, *111*, 3669.
(27) Xu, H. X.; Aizpurua, J.; Käll, M.; Apell, P. *Phys. Rev. E* **2000**, *62*, 4318.
(28) Wei, H.; Hao, F.; Huang, Y. Z.; Wang, W. Z.; Nordlander, P.; Xu, H. X. *Nano Lett.* **2008**, *8*, 2497.
(29) Ru, E. C. L.; Etchegoin, P. G.; Meyer, M. *J. Chem. Phys.* **2006**, *125*, 204701.
(30) Lee, S. J.; Morrill, A. R.; Moskovits, M. *J. Am. Chem. Soc.* **2006**, *128*, 2200.
(31) Camargo, P. H. C.; Rycenga, M.; Au, L.; Xia, Y. N. *Angew. Chem., Int. Ed.* **2009**, *48*, 2180.
(32) Li, J. F.; Huang, Y. F.; Ding, Y.; Yang, Z. L.; Li, S. B.; Zhou, S.; Fan, F. R.; Zhang, W.; Zhou, Z. Y.; Wu, D. Y.; Ren, B.; Wang, Z. L.; Tian, Z. Q. *Nature* **2010**, *464*, 392.
(33) Hosono, E.; Matsuda, H.; Honma, I.; Ichihara, M.; Zhou, H. S. *Langmuir* **2007**, *23*, 7447.
(34) Sato, S.; Nakamura, R.; Abe, S. *Appl. Catal., A* **2005**, *284*, 131.
(35) Rhee, C. H.; Lee, J. S.; Chung, S. H. *J. Mater. Res.* **2005**, *20*, 3011.
(36) Huang, L. H.; Sun, C.; Liu, Y. L. *Appl. Surf. Sci.* **2007**, *253*, 7029.
(37) Guo, W.; Shen, Y. H.; Boschloo, G.; Hagfeldt, A.; Ma, T. L. *Electrochim. Acta* **2011**, *56*, 4611.
(38) Chen, X. W.; Sandoghdar, V.; Agio, M. *Nano Lett.* **2009**, *9*, 3756.
(39) Ming, T.; Zhao, L.; Yang, Z.; Chen, H. J.; Sun, L. D.; Wang, J. F.; Yan, C. H. *Nano Lett.* **2009**, *9*, 3896.
(40) Yang, Z. L.; Li, Y.; Li, Z. P.; Wu, D. Y.; Kang, J. Y.; Xu, H. X.; Sun., M. T. *J. Chem. Phys.* **2009**, *130*, 234705.
(41) Tompkins, H. G. *J. Appl. Phys.* **1991**, *70*, 3876.
(42) Johnson, P. B.; Christy, R. W. *Phys. Rev. B* **1972**, *6*, 4370.